

Structural properties of bi-layer Molybdenum Thin-film deposited by RF magnetron sputtering for CZTS solar cells

A.K.S.Gupta¹, E.M.K.I.Ahamed¹, M. Quamruzzaman¹, M. A. Matin¹, K.S. Rahaman², N. Amin²

¹Chittagong University of Engineering and Technology (CUET), Bangladesh.

²Institute of Sustainable Energy, Universiti Tenaga Nasional (@The National Energy University), Jalan IKRAM-UNITEN, 43000 Kajang, Selangor, Malaysia

Abstract—CZTS (Copper Zinc Tin Sulfide) is a propitious absorber material for photovoltaic applications and gaining popularity for its material abundances and non-toxicity. In order to get good adhesion with substrate and at the same time low film resistivity, bi-layer Molybdenum (Mo) thin-films are frequently used as back electrode in substrate-structured CZTS based Thin-film Solar Cells (TFSCs). In a bi-layer structured Mo film, usually a thin high-pressure (HP) bottom layer serves to give better adhesion and a thick low-pressure (LP) top layer shown lower film resistivity. In this work, structural study of two different stacks (total 1 μ m film thickness) of HP layer and LP layer for both as-deposited and Vacuum Thermal Annealing (VTA) @560°C for 45 minutes were performed. Crystals were more oriented along [200] plane instead of [110] plane and oxidation at the Mo surface were observed for thicker bottom layer. It has been found that, for thinner bottom layer, not only increased crystallite size (from 19.27 nm to 21.26 nm for as-deposited and VTA treated case respectively), but also compressive stressed Mo films were found. It is evident that this bi-layer Mo thin-film is suitable for CZTS solar cell fabrication.

Keywords—RF sputtering; bi-layer Mo thin-film, vacuum thermal annealing; oxidation; compressive stress.

I. INTRODUCTION

Historically Molybdenum (Mo) is used as rear electrode for Chalcopyrite based Thin-Film Solar Cells (TFSCs) e.g. CIGS(Se) since long time [1,2]. Sputtered deposition of Mo films is the best choice. Among the two sputter deposition processes, for instance, DC and RF, researchers around the world performed a plenty of work in depositing Mo films as a rear electrode with the advent of Chalcopyrite and Kesterite based TFSCs. Although other materials as a back contact electrode tried in some innovative works, [3] but none performed well than Mo. Some specific features make Mo as a unique choice like films having low resistivity, high thermal stability, and mechanically rigid [4]. As Kesterite based TFSCs e.g. CZTS(Se) adopted from its closer cousin Chalcopyrite based TFSCs, Mo captured its candidacy as a rear contact electrode in substrate-structured pure sulphide, selenium or sulfo-selenium based Kesterite TFSCs. Researchers found that,

in order to get two desirable properties simultaneously, to illustrate, adhesion with glass substrate and film's low sheet resistivity is a tedious job by magnetron sputtering. Revolutionary work done by Scofield et al. [5] first put the bricks on the highway towards the goal to acquire Mo films' adhesion and low resistivity properties using the concept of bi-layered film deposition by DC magnetron sputtering. A thin bottom layer (adhesion layer) followed by a thick top layer (low resistivity layer) upon the variation of Argon (Ar) pressure, HP for bottom and LP for top were proposed and successfully had been utilizing the recipe by NREL researchers till date. After that, using this bi-layered Mo thin-film deposition concept, researchers opened the door using RF magnetron sputtering as well [6, 7]. Both RF and DC deposited films showed similar trends in microstructural evolution and the strain in the film varied in a similar fashion, transitioning from compressive through tensile and back to compressive again [8]. In terms of adhesivity, minor disparities were observed for RF and DC sputtered Mo films. Conductivity of RF sputtered films found lower than that of DC sputtered films indicating the presence of alien atoms, which contributed to increase series resistance, particularly harmful for both hard and flexible substrates [9]. When the Mo films were grown on SLG substrate followed by absorber layer and as absorber layer had to undergo a high-temperature annealing process, Mo sandwich layer then served as a gateway to diffuse Sodium (Na) from SLG substrate to absorber contributed to larger grain size [10]. As DC sputtered Mo films found with larger grain size as compared to RF sputtered, from the beginning, it was less advantageous for Na diffusion; attracting researchers to deposit Mo films by RF magnetron sputtering. Moreover, interfacial layer, MoS_x formed during absorber annealing and Na diffusion or doping is one of the controlling parameters to keep the MoS_x layer thickness optimum; RF magnetron sputtering Mo films can do it well.

II. EXPERIMENTAL DETAILS

Bi-layered Molybdenum (Mo) thin-films were RF magnetron sputtered onto 3cm×3cm×1.2mm Corning® soda lime glass (SLG) substrates using Nanomaster Inc. USA NSC-3500 RF (13.56 MHz) magnetron sputter coater system. The

diameter of the Mo target was 2 inch having purity 99.99% with a copper backing plate and keeper. The distance between the Mo target and substrate holder was kept at 9cm for all investigations. The SLG substrates were ultrasonically cleaned using sequential MAMD (Methanol-Acetone-Methanol-DI water) process prior to cleaning with soap solutions. Ultrasonically cleaned substrates were then dried by Nitrogen (N₂) jet stream. Plasma cleaning of Mo target was performed by pre-sputtering for 30-minutes under vacuum when shutter is in closed position before starting deposition. The sputtering machine is software interfaced with computer, so all needed sputtering parameters and recipes can be set using keyboard inputs. The base pressure was set at 6.7 mPa. The working pressure was adjusted for varying Ar flow rate (SCCM), for instance, at 0.88 Pa when using high pressure (HP) and at 0.30 Pa for low pressure (LP) sequence respectively. No intentional substrate heating was applied during deposition. The RF power and substrate rotation were set to 100W and 10rpm respectively. The thicknesses of the deposited films were recorded by system incorporated QCM (Quartz Crystal Monitor) whose tooling factor was calibrated earlier for Mo deposition by setting material density and Z-factor. Moreover, deposited film thicknesses were double checked by measuring by Dektak profilometer. Structural properties were assessed by XRD which uses CuK α radiation having wavelength, $\lambda=1.5408 \text{ \AA}$. We used Scherrer formula as in (1) [11] in order to tabulate averaged crystallite sizes (D) of the deposited films.

$$D=0.9\lambda/\beta\cos\theta \quad (1)$$

Where, λ is the wavelength of CuK α radiation (0.15406 nm), and β is the full width at half maximum [FWHM] of the fabricated film in radian at which angle the diffraction peak occurs and θ is the Bragg's diffraction angle in degree. The microstrain, ϵ and dislocation density, δ developed in the films are calculated from equations as in (2) and (3) respectively [12, 13]

$$\epsilon=\beta/4\tan\theta \quad (2)$$

$$\delta=n/D^2 \quad (3)$$

Where, n is a factor, which is practically equivalent to unity for least dislocation and D is the grain size.

Adhesion tests were performed by scotch tape. Vacuum Thermal Annealing (VTA) @ 560°C for 45 minutes were set and put the samples inside a quartz tube under N₂ flux. GSL-1100X Thermal Annealer, MTI corporation, USA were used.

III. RESULTS AND DISCUSSIONS

The structural properties of bi-layer Mo films are analyzed for both as-deposited and VTA treated conditions.

A. Structure and adhesion

Bi-layered Mo thin-films were deposited by RF magnetron sputtering technique on SLG substrate. Structural studies were performed for two cases as depicted in Fig. 1. The bottom layer was deposited at HP (0.88Pa) while the top layer was deposited at LP (0.30 Pa) for different time to achieve appropriate layer thickness. The overall thickness of the bi-layer Mo thin-film stacks was approximately 1000nm.

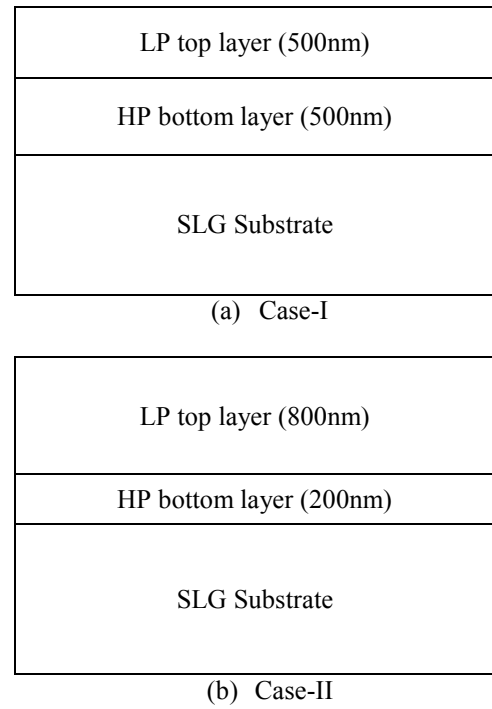


Fig.1. Schematic of the bi-layer Mo rear contact (not drawn in scale). (a) 500nm HP bottom layer and 500nm LP top layer and (b) 200nm HP bottom layer and 800nm LP top layer

The sputter deposited bi-layer Mo films are shown in Fig.2. For both cases, in these investigations, deposited Mo films were passed the Scotch-tape tests as shown in Fig.3. Although no peel-off of films observed, minor pin-holes at some places were seen.

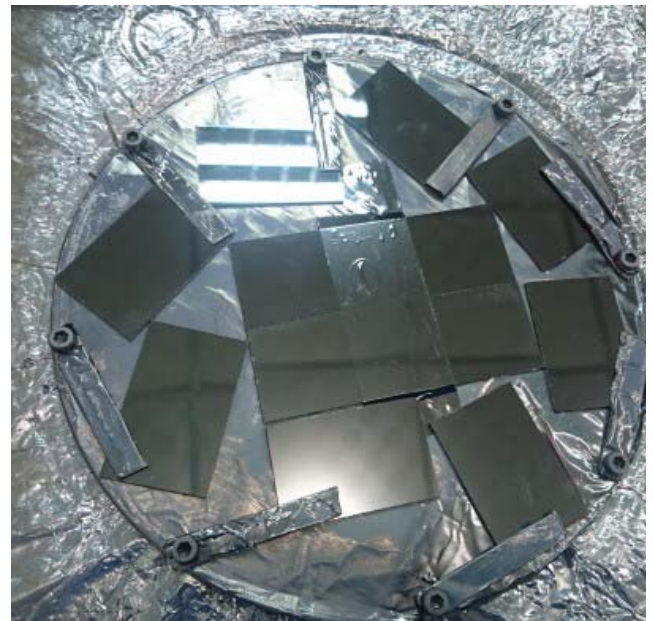


Fig.2. Sputter deposited bi-layer Mo films.



Fig.3. Mo thin-film adhesion tests

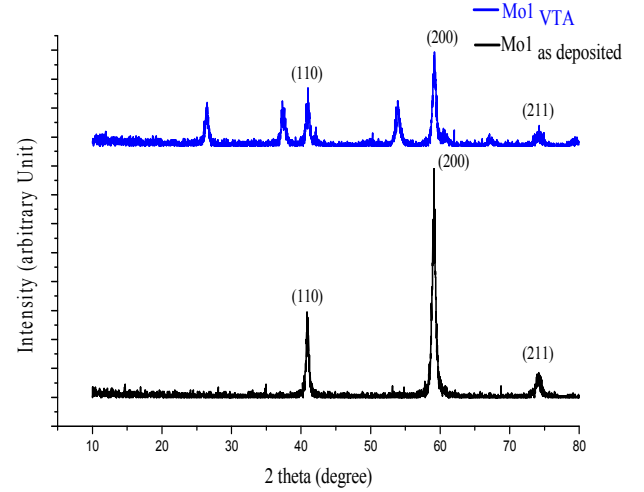


Fig.4. XRD patterns of Mo thin films for case-I (as deposited and VTA treated). Other unlabeled peaks are associated with Mo oxide phases.

B. Crystallinity and Microstructure

The XRD spectrums of bi-layer Mo thin-films fabricated in this study are agreed with standard JCPDS card no. 65-7442. The result indicates that, the fabricated bi-layer Mo thin-films are crystalline in nature and crystallizes in body-centered cubic (BCC) structure corresponding to space group symbol $Im\bar{3}m$ and group number 299 [14].

Case-I

The structural properties and crystallinity of the Mo back contact electrode stacks was studied by XRD measurements. For this particular case, three pronounced peaks with corresponding 2θ values centered at 40.88° , 59.12° , 74.16° were found and indexed as Mo [110], Mo [200], Mo [211] respectively for as-deposited study i.e. before VTA treatment.

After VTA treatment for the case under study, multiple Bragg's peaks other than [110], [200], [211] planes were observed. The dominant peak which was at [110] plane for as-deposited case found to be at [200] plane indicating preferential orientation of crystal structure had been changed. Other un-labeled peaks were associated with MoO_x phases.

Bragg's peak intensity at Mo [110] plane found lower for annealed case pointing poor crystallinity; moreover, Mo [110] peak under annealed case shifts around 0.10° towards right which is not desirable, as will be explained in details for Case-II.

The XRD patterns are shown in Fig.4. The average crystallite size, Lattice constant, Microstrain and Dislocation density for Case-I also calculated and summarized in TABLE-I. The crystallite size of annealed film were found surprisingly reduced (13.79 nm to 12.75 nm) than as-deposited with corresponding increase in FWHM from 0.55° to 0.63° , suggesting hard to accept bi-layered stack sequence with mentioned thicknesses for Case-I.

TABLE I. CRYSTALLOGRAPHIC DATA OF SPUTTER DEPOSITED BI-LAYER MO FILMS (CASE-I)

Sample	Peak position at [110] plane, 2θ	Average crystallite size, nm	Lattice constant, (Å^0)	Micro strain, ϵ ($\times 10^{-3}$)	Dislocation density, δ ($\times 10^{12}$)
Mo1_as deposited	40.88°	13.79	3.12	5.42	1.89
Mo1_VTA	40.98°	12.45	3.12	7.49	2.89

Case-II

For this case, all the patterns showed a dominant XRD peak at [110] plane. Specifically, there were two significant peaks at [110] and [211] planes for both as-deposited and VTA treated case but peaks at [200] plane was almost negligible. The FWHM of the [110] oriented plane is reduced from 0.36° to 0.34° after VTA treatment signifying increased grain size of Mo films. The intensity of [110] peak also swelled significantly. The phenomena of swelling intensity and shrinking FWHM at [110] Bragg's peak clearly pointed the improvement of crystallinity after VTA process. As an upshot, grain size increased from 19.27nm to 21.26nm. The peak at [110] plane after VTA treated bi-layered Mo-film slightly shifted left around 0.04° , stipulated the modification of the average lattice spacing in the direction normal to the plane of the film, which agreed with the results found by [15]. Left shift in angle means large lattice spacing in the direction normal to the surface, which dictates Mo bi-layer becomes more compressive after VTA treatment. This compressive stress helps in getting more dense Mo films, which were absent in our studied result found for Case-I.

The XRD patterns are shown in Fig.5. The average crystallite size, Lattice constant, Microstrain and Dislocation density for Case-II also calculated and summarized in TABLE-II. The

crystallite size of annealed film were increased (19.27 nm to 21.26 nm) than as-deposited with corresponding decrease in FWHM from 0.36° to 0.34°, suggesting bi-layered stack sequence with mentioned thicknesses for Case-II, would be favorable for full cell fabrication.

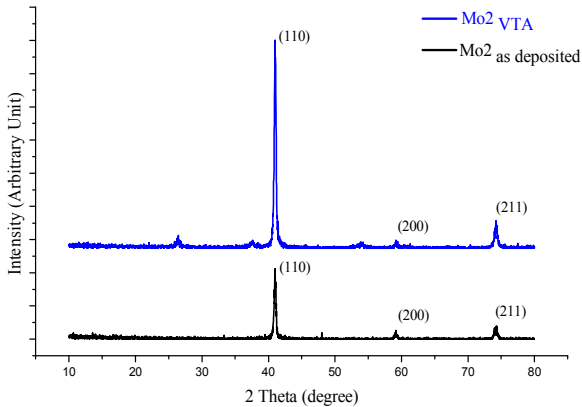


Fig.5. XRD patterns of Mo thin films for case-II (as deposited and VTA treated).

TABLE II. CRYSTALLOGRAPHIC DATA OF SPUTTER DEPOSITED BI-LAYER MO FILMS (CASE-II)

Sample	Peak position at [110] plane, 2θ	Average crystallite size, nm	Lattice constant, (Å)	Micro strain, ϵ ($\times 10^{-3}$)	Dislocation density, δ ($\times 10^{12}$)
Mo2_as deposited	41.02°	0.36°	19.27	3.12	3.89
Mo2_VTA	40.98°	0.34°	21.26	3.12	3.61

IV. CONCLUSIONS

In this investigation, the prime goal was to perform structural studies of two different stack thicknesses of bi-layered Mo thin-films to be used as a back contact electrode in CZTS TFSCs. For Case-I, each 500nm thick HP and LP layers (1 μm thick in total) bi-layered Mo thin-film were considered. For Case-II, 200nm thick HP bottom layer and 800nm thick LP top layer were fabricated. Adhesion tape tests were successfully passed for each case. Case-I resulted in oxidation at Mo surface along with Mo phases in other planes after VTA treatment. Neither the crystallinity nor the compressive stress found better for Case-I. Moreover, it showed intensified preferred orientation of Mo along [200] plane instead of [110]. But for Case-II, better crystalline orientation was obtained along [110] plane, increased grain size from 19.27 nm (as-deposited) to 21.26 nm (VTA), densely compressive stressed films were found. Overall result suggested that thin HP bottom layer will ensure better adhesion, crystallinity and denser films to be used as a back contact electrode in high-performance CZTS thin-film solar cells.

ACKNOWLEDGMENT

We would like to acknowledge the characterization support provided by UKM (Universiti Kebangsaan Malaysia), Malaysia.

REFERENCES

- [1] G. Francesco Biccari, Rosa Chierchia, Matteo Valentini, Pietro Mangiapane, Enrico Salza, Claudia Malerba, Cristy Leonor Azanza Ricardo, Loredana Mannarino, Paolo Scardi, Alberto Mittiga, "Fabrication of $\text{Cu}_2\text{ZnSnS}_4$ solar cells by sulfurization of evaporated precursors," *Energy Procedia* 10 (2011), p.p.187 – 191.
- [2] Philip Jackson, Dimitrios Hariskos, Erwin Lotter, Stefan Paetel, Roland Wuerz, Richard Menner, Wiltraud Wischmann and Michael Powalla, "New world record efficiency for $\text{Cu}(\text{In,Ga})\text{Se}_2$ thin-film solar cells beyond 20%," *Prog. Photovolt: Res. Appl.* 2011;19:894–897
- [3] K. Orgassa, H.W. Schock, J.H. Werner, "Alternative back contact materials for thin film $\text{Cu}(\text{In,Ga})\text{Se}_2$ solar cells," *Thin Solid Films*, 431 – 432(2003), pp.387–391
- [4] Mukter zaman, Gunawan Witjaksono, Teh Aun Shih, Shabui Islam, Masuri Othman and Nowshad Amin, "The Effect on Physical, Electrical and Structural Parameters of RF Sputtered Molybdenum Thin Film," *Advanced Materials Research Vols. 403-408* (2012), p.p. 5092-5096
- [5] John H. Scofield, A. Duda, D. Albin, B.L. Ballardb, P.K. Predeckib, "Sputtered molybdenum bilayer back contact for copper indium diselenide-based polycrystalline thin-film solar cells," *Thin Solid Films* 260 (1995) 26-31
- [6] P. Chelvanathan, S.A. Shahahmadi, F. Arith, K. Sobayel, M. Aktharuzzaman, K. Sopian, F.H. Alharbi, N. Tabet, N. Amin, "Effects of RF magnetron sputtering deposition process parameters on the properties of molybdenum thinfilms," *Thin Solid Films* 638 (2017), pp.213–219
- [7] H. Khatri and S. Marsillac, "The effect of deposition parameters on radiofrequency sputtered molybdenum thin films," *J. Phys.: Condens. Matter*, 20(2008).
- [8] K. Aryal, H. Khatri, R. W. Collins, S. Marsillac, "In Situ and Ex Situ Studies of Molybdenum Thin Films Deposited by rf and dc Magnetron Sputtering as a Back Contact for CIGS Solar Cells," Hindawi Publishing Corporation, *International Journal of Photoenergy*, Volume 2012, Article ID 723714, 7 pages, doi:10.1155/2012/723714
- [9] E. Eser, S. Fields, G. Hanket, R. W. Birkmire and J. Doody, "Critical issues in vapor deposition of $\text{Cu}(\text{InGa})\text{Se}_2$ on polymer web: source spitting and back contact cracking," *Conference Record of the Thirty-first IEEE Photovoltaic Specialists Conference, 2005.*, Lake Buena Vista, FL, USA, 2005, pp. 515-518.
- [10] Akira Nagaoka, Hideto Miyake, Tomoyasu Taniyama, Koichi Kakimoto, Yoshitaro Nose, Michael A. Scarpulla, Kenji Yoshino, "Effects of sodium on electrical properties in $\text{Cu}_2\text{ZnSnS}_4$ single crystal," *Applied Physics Letters* 104, 152101 (2014)
- [11] A. L. Patterson, "The Scherrer Formula for X-Ray Particle Size Determination," *Phys. Rev.* 56, 978
- [12] G.K. Williamson, W.H. Hall, "X-ray line broadening from filed aluminium and wolfram," *Acta Metallurgica*, Volume 1, Issue 1, January 1953, p.p. 22-31.
- [13] G. K. Williamson, R. E. Smallman, "Dislocation densities in some annealed and cold-worked metals from measurements on the X-ray debyescherrer spectrum," *Philosophical Magazine*, 1:1, p.p. 34-46.
- [14] Joint Committee on Powder Diffraction Standards (JCPDS), cards no. 65-7442.
- [15] Xiaolei Liu, Hongtao Cui, Charlie Kong, Xiaojing Hao, Yidan Huang, Fangyang Liu, Ning Song, Gavin Conibeer, Martin Green, "Rapid thermal annealed Molybdenum back contact for $\text{Cu}_2\text{ZnSnS}_4$ thin film solar cells," *Applied Physics Letters* 106, 131110 (2015)